

ORIGINAL ARTICLE

Investigating the Effect of Shape on Acoustic Performance of Micro Perforated Absorber at Low Frequencies

MOHAMMAD REZA MONAZZAM¹, ZAHRA HASHEMI^{2*}

¹*School of Public Health and Center for Air Pollution Research (CAPR), Institute for Environmental Research (IER), Tehran University of Medical Sciences, Tehran, Iran*

²*Behbahan Faculty of Medical Sciences, Behbahan, Iran*

Received April 17, 2019; Revised June 10, 2019; Accepted August 11, 2019

This paper is available on-line at <http://ijoh.tums.ac.ir>

ABSTRACT

Nowadays, micro-perforated absorbers are one of the structures that are widely used. The sound absorption mechanism is performed by viscous energy losses in the cavities on the plate. This paper was examined the effect of the surface shape on the micro-perforated absorber performance at low frequencies (less than 500 Hz). The three-dimensional finite element method was used to predict the absorption coefficient of this group of adsorbents. Also, the results obtained from the shaped absorbers were compared with the flat micro-perforated absorbers. After validating the numerical results, six different designs were defined as the surface shape of the micro-perforated plates in the COMSOL Multiphysics, Ver. 5.3a software. The results reflected the fact that the factor of the surface shape can be used as a contributing factor in some frequencies. In general, the dented or concave shapes provided better outcomes than other flat designs and shapes and the convex or outward shapes bring the weakest results.

Keywords: *Micro-Perforated Absorbers, Surface Shapes, Low Frequency, Absorption Coefficient*

INTRODUCTION

The progress of the industry over the past 60 years has been accompanied by an increasing index in pollutants such as air, water, visual, and noise pollutions. Although, noise pollution is an integral part of urban life, meanwhile, the impact of excessive exposure to sound can cause problems, one of the most common is hearing loss [1]. According to the World Health Organization, the number of people suffering from hearing loss all over the world has increased from 120 million in 1995 to 250 million in 2004 [2]. Continuous and long-term exposure to sound pressure levels can lead to quantitative and qualitative

understanding of the warning signs [3]. Other side effects may include increased risk of accidents [3], disruptions in communication with individuals resulting in the lack of proper and effective effects may include increased risk of accidents [3], increased stress, increased blood pressure [4], increased heart rate [5], psychological injuries [6-7], distress, sleep disturbances, and increased cardiovascular diseases [8]. To prevent these problems, an adaptation needs to be made among the standards of sound and technology, transportation, worksites, and recreational facilities, which can be done in various ways such as upgrading the machinery, vehicles replacement,

Corresponding author: Zahra Hashemi

E-mail: Z.hashemi26@yahoo.com

design, and construction of new indoor environments or noise control protocols.

Noise control can be done in various forms such as controlling at the source, controlling at the receiver, and controlling in the sound propagation path. When the goal is to control the noise in the path of propagation, the issue of reduction in the reverberation time comes to the focus of attention. Reducing the reverberation time includes the control of noise transferred through the air, known as the airborne noise. One of the methods of noise control is the absorption phenomenon. Acoustic materials are typically designed for noise absorption. The passive absorbers are effective at mid and high frequencies, where the ear has a high sensitivity. However, the noise control in the spectrum of low frequencies seems still problematic. This type of sound occurs in a range of frequencies that is less diminished by walls or other structures. It can also mask higher frequencies and travel longer distances just with a bit reduction. Other features of low-frequency noise are the creation of resonance in humans and the development of mental and, to some extent, physiological responses [9]. These complications include tinnitus, headache, increased level of cortisol secretion, increased stressful reactions, respiratory impairments, sense of discomfort, and complaints [10-11]. The equipment and devices involved in generating low-frequency noise may include the followings: internal combustion engines, compressors, fans and blowers, power transformers, gearboxes, ventilation devices, computer network facilities, control rooms in different industries, diesel engines, office-work environments, roads and highways traffic, sewage pipelines path, ionizing beam production equipment, pumps and washing machines, boilers, refrigerators, and cooling towers [9].

The perforated plates have been successfully used so far as absorbers in many buildings [12-13], medical equipment [14], and mufflers [15-16]. A micro-perforated absorber typically contains a perforated plate, which is placed with a distance from a rigid wall. The sound absorption mechanism is performed by viscous energy losses in the cavities on the plate. When the size of the cavities is reduced, these classes of absorbers gain a high resistance and low reactance, which provides them the required conditions to become suitable absorbers with a broad absorption spectrum. This structure provides better

performance than other resonance structures [17]. However, it provides a weaker performance in comparison with the porous material both in terms of frequency bandwidth and the absorption rate. Many studies have been done on effective factors that were aimed to increase the acoustic performance of this category of absorbent materials in recent years. Some of these studies include compartmentalizing the space behind the plate and creating spaces with different depths [18], the use of two consecutive perforated plates [19], the use of multi-layer micro-perforated plates [20-21], and the use of absorbent materials behind the plate [22]. In some studies, the resonance of the same micro-perforated structure has been used, especially at low frequencies [23-24].

The surface shape of these materials is one of the factors affecting the acoustic behavior of the absorbent materials. Few studies have looked at the apparent shape of the adsorbent materials. For example, Chens examined the effect of the shape of porous absorbers behind the micro-perforated plate. He examined the simple, semicircular, concave, and triangular shapes and concluded that the form of porous absorbers definitely affects the absorption coefficient at some frequencies [25]. Easwaran et al. studied the sound reflection coefficient from the foam edges using the Galerkin finite element method [26]. Kang et al. investigated the rates of absorption coefficient and sound transmission loss in the panel composite structure by the finite element method [27]. The results of both studies revealed that the porous materials with an edged shape improve the rates of absorption coefficient and the transmission loss in some frequency bands. Also, Tsay et al. conducted research on exploring the acoustic absorption rate of polyurethane foams with pyramidal surface geometry. Different dimensions of pyramidal geometry of polyurethane foam with different vertex angles were analyzed, which the results showed that the highest absorption coefficient has been obtained at a vertex angle of 29°. According to the conducted research, it seems that few studies have focused on the appearance of absorbers, particularly the micro-perforated absorbers. Therefore, in the current study, the effect of the surface shape on the performance of micro-perforated absorbers using the finite element method was evaluated [28].

METHODS

The theoretical part of the finite element method

To explain the acoustic performance of the perforated plate, it was assumed that the sound wave is emitted from the sound source with a “tetha” angle and creates an azimuth beta angle in impacting the plate. A part of the acoustic energy of the wave was dispersed and a part of it was absorbed by the micro-perforated plate. The finite element method in the frequency domain to simulate the acoustic performance was used. The computing range included the space behind the micro-perforated plate, the micro-perforated plate itself, and a virtual channel. The sound field in the backspace and the air passageway was satisfied by solving the Helmholtz equation.

$$(\nabla^2 + K_0^2)\phi = 0 \quad (1)$$

Here, $k = \omega/c_0$ is the number of wave in the free field and ϕ is the velocity potential, which is related to the sound pressure and the acoustic velocity of the particles (\mathbf{u}).

$$P = -i\rho_0\omega\phi, \mathbf{u} = \nabla\phi. \quad (2)$$

The ρ_0 , c_0 are the density and speed of sound in the air and ω represents the angular frequency, respectively. Also, $i = \sqrt{-1}$ represents the imaginary numbers. By ignoring the vibration of the plate, the page, itself, has been placed in the Neyman boundary conditions group.

$$\frac{\partial\phi}{\partial Z} = \frac{P_{cav} - P_{duct}}{\rho_0 C_0 Z} \quad (3)$$

Here, p_{cav} and p_{duct} refer to the air pressure in the back compartment and the air passage channel, respectively, while Z is the acoustic impedance of the micro-perforated plate relative to the air, obtained according to Maa's formula [29] Z can be determined using Equation 4:

$$Z = \frac{32\eta t}{\sigma\rho_0 C_0 d^2} \left[\left(1 + \frac{k^2}{32}\right)^{1/2} + \frac{\sqrt{2}}{32} K \frac{d}{t} \right] + i \frac{\omega t}{\sigma C_0} \left[1 + \left(9 + \frac{K^2}{2}\right)^{-1/2} + 0.85 \frac{d}{t} \right] \quad (4)$$

And here

$$K = d \sqrt{\omega\rho_0/4\eta}$$

Where,

d : orifice diameter, t : thickness of the panel, η : viscosity coefficient, and σ : perforation ratio in percentage.

A Dirichlet-to-Neumann boundary conditions [30] was used in the virtual channel input section cause the sound wave to cross this border without reflection. The implementation of boundary conditions in 3D geometry was described as below. The total pressure at the entrance of the virtual channel includes the input wave pressure and the pressure of the dispersed wave, or in other words:

$$\phi = \phi_{in} + \phi_{sc}. \quad (5)$$

Given the coordinates stated in Figure 1, the input wave pressure can be written as follows:

$$\phi_{in} = e^{i(k_x x + k_y y + k_z z)} \quad (6)$$

The wave numbers in different directions can be written as follows:

$$k_x = k_0 \sin \theta \cos \beta \quad (7)$$

$$k_y = k_0 \sin \theta \sin \beta \quad (8)$$

$$k_z = k_0 \cos \theta \quad (9)$$

The acoustic pressure absorbed by the micro-perforated plate can be calculated as follows:

$$\begin{aligned} P_{abs} &= - \iint_{S_{inlet}} Re(pu_z^*) dx dy \\ &= \rho_0 \omega \iint_{S_{inlet}} Re \left[(i\phi) \left(\frac{\partial \phi}{\partial Z} \right)^* \right] dx dy, \end{aligned} \quad (22)$$

The star sign refers to the complexity of the phrase. Regarding the input wave pressure, the acoustic input power in Equation 6 is as follows:

$$P_{in} = \rho_0 \omega k_0 (\cos \theta) L_x L_y \quad (23)$$

The oblique incidence absorption coefficient is the ratio of the diffused wave pressure to the absorbed wave pressure, which can be written as follows:

$$\alpha_{\theta, \beta} = \frac{\iint_{S_{inlet}} Re \left[(i\phi) \left(\frac{\partial \phi}{\partial Z} \right)^* \right] dx dy}{k_0 (\cos \theta) L_x L_y} \quad (24)$$

After validating the numerical results based on the experimental results [22], there were many designs ranging from complex to simple shapes in order to examine the effect of the surface shape on the

absorbance performance of micro-perforated absorbers.

Factors to consider in this study were the simplicity of the designs both in terms of drawing in software and in the construction and use phase as well as aesthetics and decoration issues. Therefore, the designs provided below were selected as the surface shape of the micro-perforated plate. A flat micro-perforated plate (A) was used as a reference for comparison. The structural characteristics of the micro-perforated plates were considered to be the same in all modes. The height behind the micro-perforated plates was a factor affecting the acoustic behavior of this group of absorbers. In the present study, the height or depth of the back compartment of the perforated plates identical and equal to 100 mm in all the designs was considered. As the plates were shaped, the depth behind the micro-perforated plate was defined by the effective height, which was obtained by integrating the volume of the back of the micro-perforated plate. The normal absorption coefficient ($\theta = 0$) was defined for adsorbents and surfaces with a flat surface. In other words, the sound wave lands on the absorber surface with an angle of zero or perpendicularly. When an absorbent surface is shaped, the acoustic wave does not practically hit the surface at a zero angle. This makes it impossible to define and calculate the normal absorption coefficient in these forms. Therefore, in this study, the oblique coefficient of absorption at the angle of $\theta = 45$ was calculated with the assumption of constant $\beta = 45$, which was then compared to the flat shape as the reference.

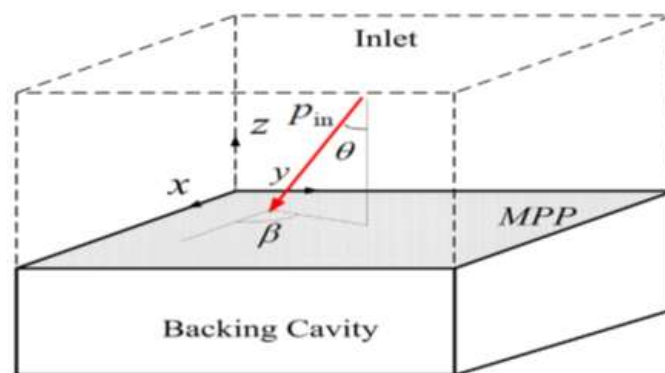
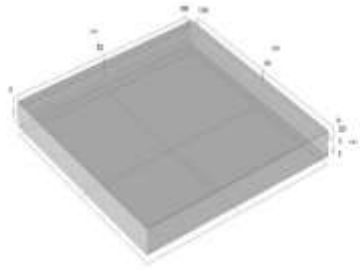
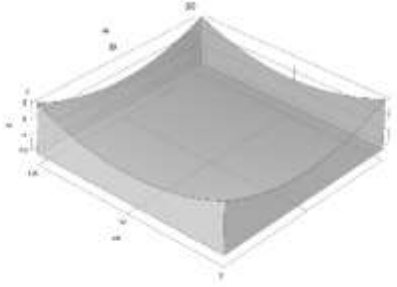
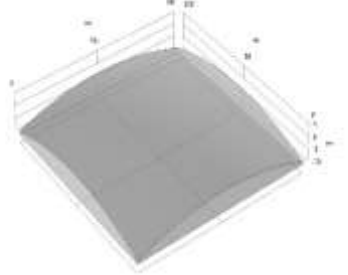
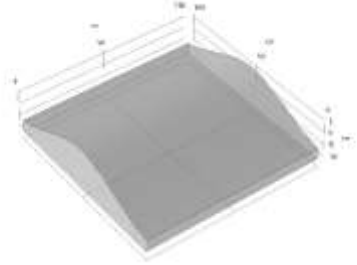
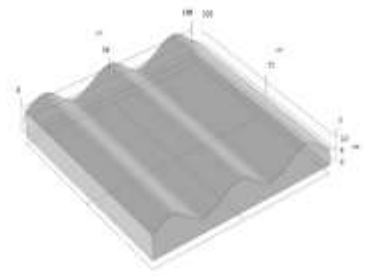
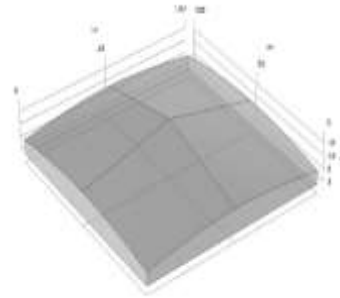


Fig. 1. Theoretical model of the MPP absorber

Table 1. The studied designs (forms) and their structural properties

Design	Max depth(mm)	Min depth(mm)	Shape
A	100	100	
B	265	1	
C	155	10	
D	155	50	
E	142	58	

F 195 50



G 165 25

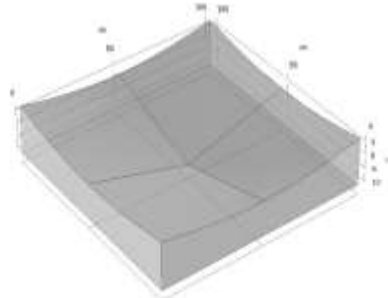


Table 2. The structural properties of Mpp

Theta	Beta	Lx	Ly	Effective Height	MPP properties	dh	tp	σ
45[deg]	45[deg]	1000[mm]	1000[mm]	100[mm]		0.5[mm]	1[mm]	0.016

Numerical results

Validation of the FEM method

To ensure the accuracy of simulation results, these results need to be compared with the results

obtained from the test or the results presented in a valid reference or an approved analytical method. To this end, the FEM simulation results in this study with the results of impedance tube in the paper were compared [22].

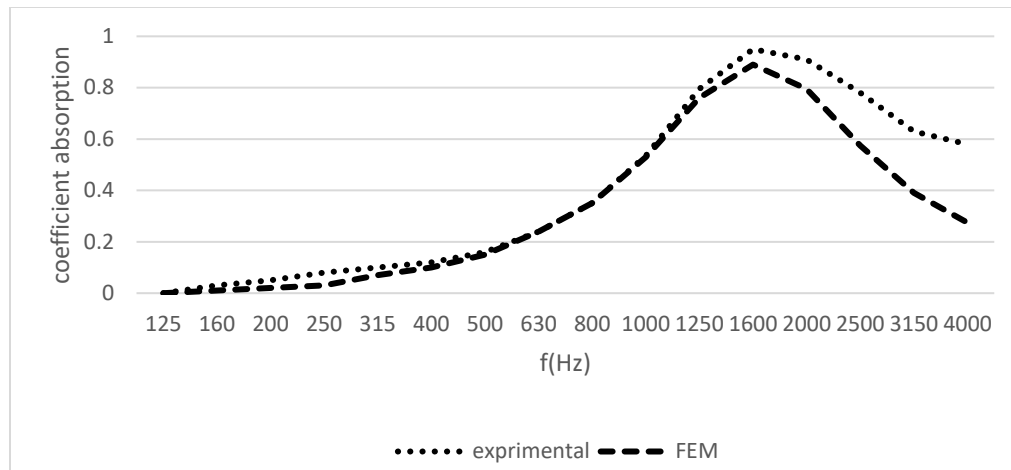


Fig. 2. Comparison between the experimental and FEM method*

*-A perforated stainless steel sheet with a thickness of 0.7 mm, the diameter of the holes 4.1mm, and a porosity percentage of 10%. Second layer: A polyurethane foam with a thickness of 10 mm and the density of 12kg/m³. Third layer: polyurethane foam with a thickness of 10 mm and the density of 25kg/m³. Fourth layer: A simple stainless steel sheet with a thickness of 0.7 mm

As shown in Figure 2, the results of both methods were somewhat close to the 1/3 octave frequency range and the graphs' trends were in perfect harmony with each other. The important point in this Figure was the closeness and similarity of the finite element method to the laboratory method at low and intermediate frequencies, while the difference between the two graphs had increased as the frequency increases. In sum, it can be concluded that this method was capable of predicting the sound performance rate of different acoustic structures.

The results of the oblique absorption coefficient rate based on the numerical method

Initially, the studied designs were drawn in the 3D environment of the COMSOL software. Then considering the appropriate boundary conditions, the oblique absorption coefficient was simulated at a 45 degrees angle at a frequency of 1 to 500 Hz. At each stage, the results of the absorption coefficient of the studied design were compared with the flat micro-perforated plate (A).

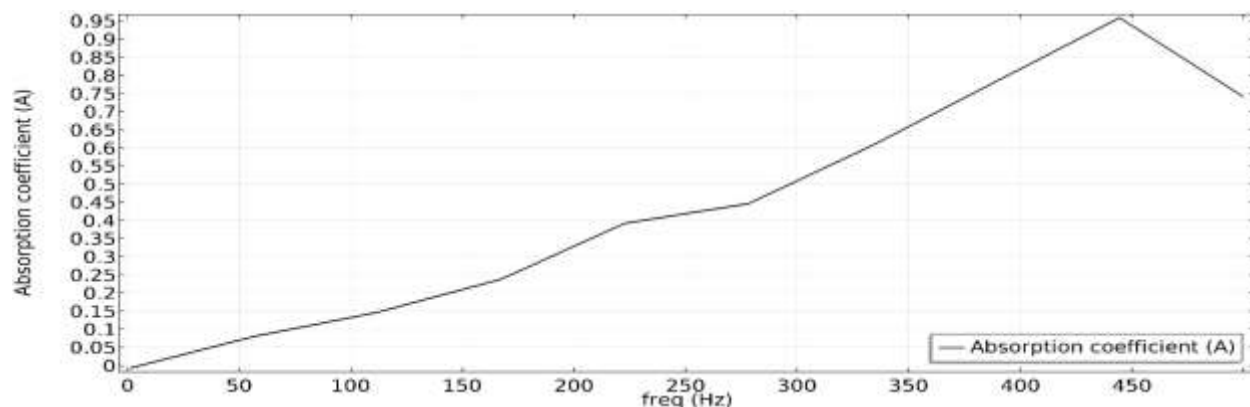


Fig. 3. Absorption coefficient of shape "A" (flat micro perforated design)

Figure 3 shows the absorption coefficient rate of shape “A”. As can be seen, the resonance frequency had occurred at 440 Hz was equal to the quantitative value of 0.95.

As it can be found, under identical conditions in terms of structure and effective depth, the design “B” or, in other words, the concave shape, had a higher

absorption coefficient than the reference shape (flat). The resonance peak in the concave micro-perforated plate had shifted to the left, i.e., the 380 Hz frequency and the quantitative value of the maximum peak were equal to 0.95, which was equal to the amount of resonance peak in the flat shape.

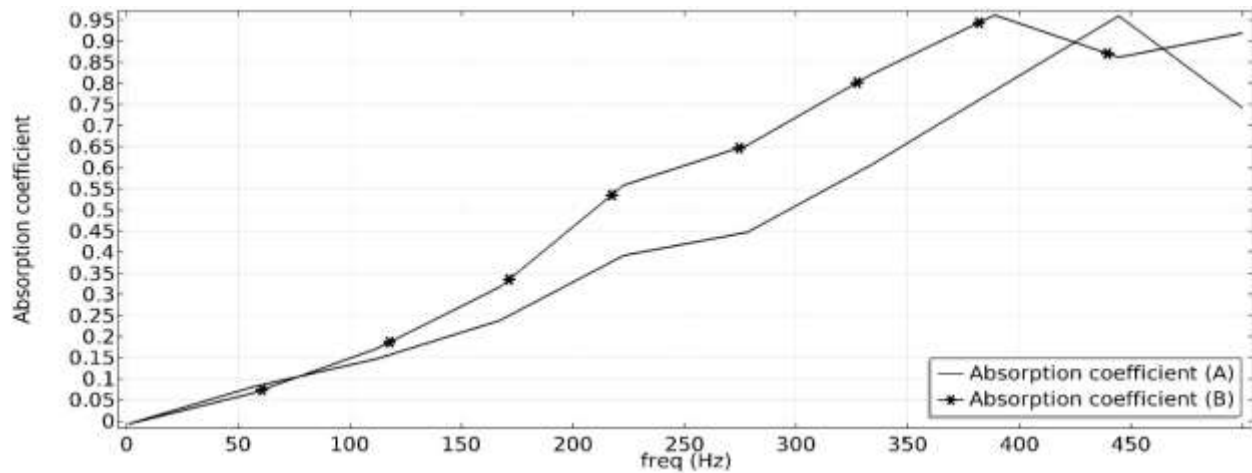


Fig. 4. Comparisons of two designs (shapes) of “A” and “B”

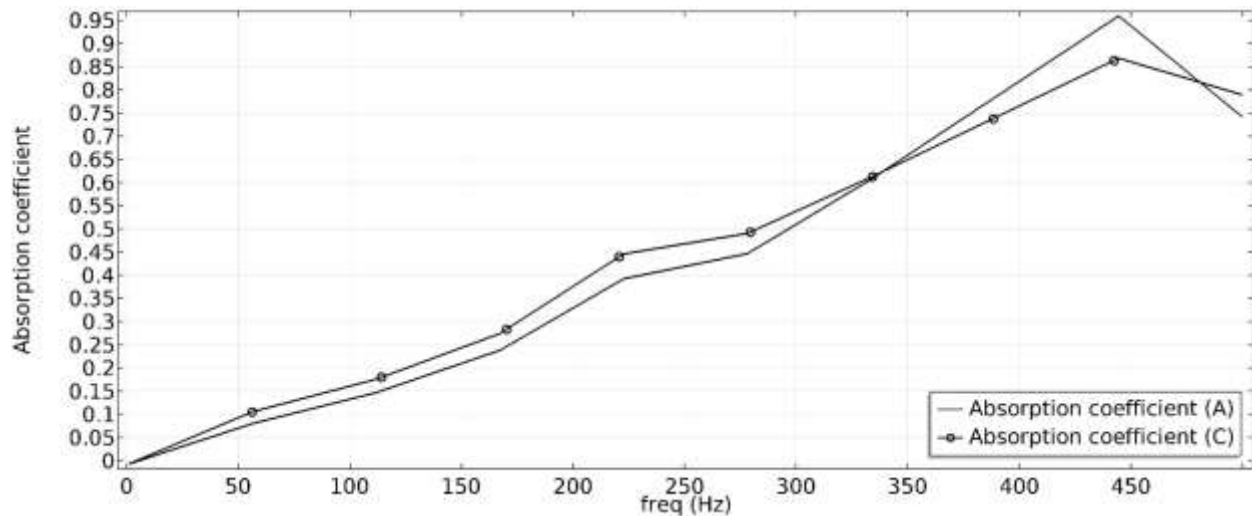


Fig. 5. Comparisons of two designs (shapes) of “A” and “C”

Figure 5 shows that there was little difference between the amount of absorption coefficient of shape “C” and the reference micro-perforated plate (A), and this difference in the frequencies below 350 Hz was in favor of the shape “C”. But its amount was negligible.

The resonance peak was identical in both designs at a frequency of about 440 Hz. In the “C” design, the absorption rate at the peak point was equal to 0.85 and less than the “A” design.

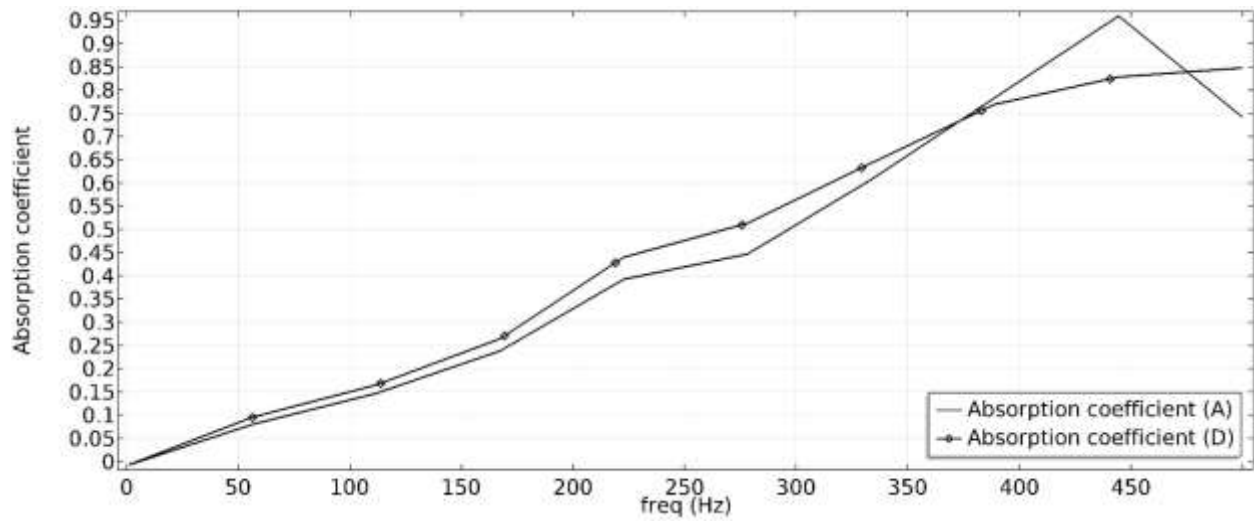


Fig. 6. Comparisons of two designs (shapes) of “A” and “D”

Figure 6 reveals that the design “D” had a better absorption coefficient than the flat micro-perforated plate at frequencies below 400 Hz. It had also a very light resonance peak at a frequency of 440 Hz with a value of 0.85.

According to the numerical results obtained from the simulation process, the two “E” and “A” designs have shown a similar behavior at frequencies below 500 Hz.

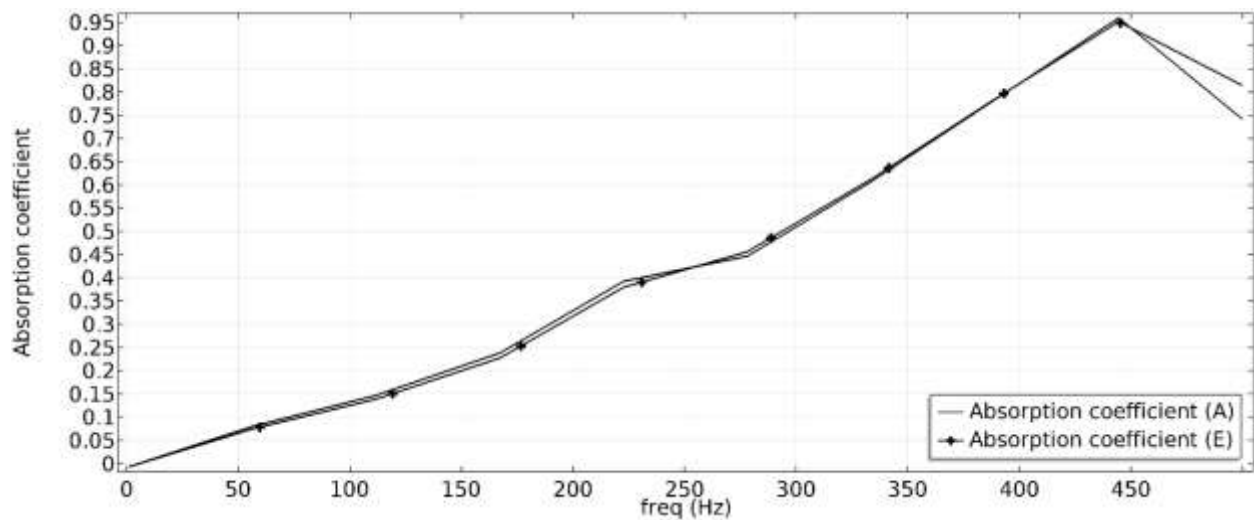


Fig. 7. Comparisons of two designs (shapes) of “A” and “E”

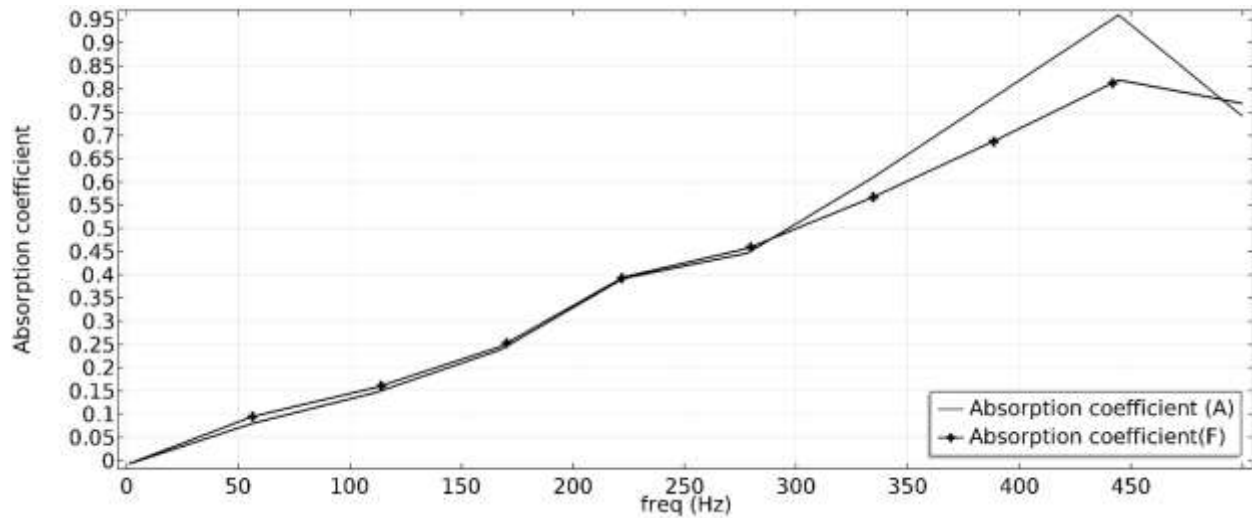


Fig. 8. Comparisons of two designs (shapes) of “A” and “F”

As it can be seen from Figure 8, the “F” shape not only had not helped the absorption coefficient but also had worsened the micro-perforated plate absorption status at some frequencies. In both shapes, the resonance

frequency was identical and equal to 440 Hz. The peak value in Figure F is 0.8, which was lower than the flat shape (0.95).

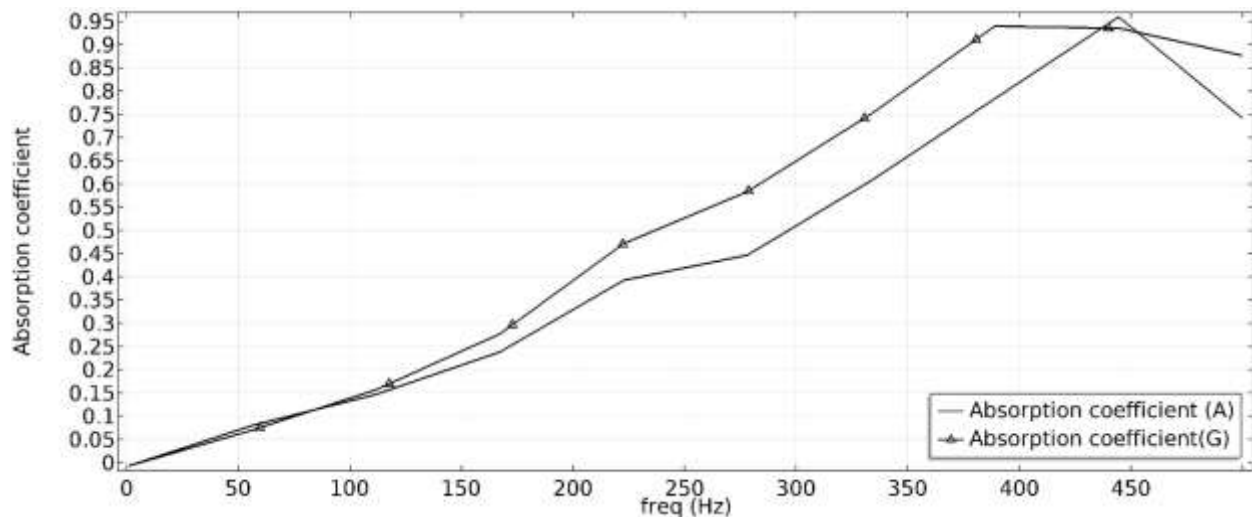


Fig.9. comparisons of two designs (shapes) of “A” and “G”

The inverse pyramid design of “G” had a higher absorption coefficient than the flat micro-perforated shape at frequencies below 430 Hz. The

resonance frequency shift to lower frequencies was evident in this shape. The absorption peak was slightly less than the design “A”.

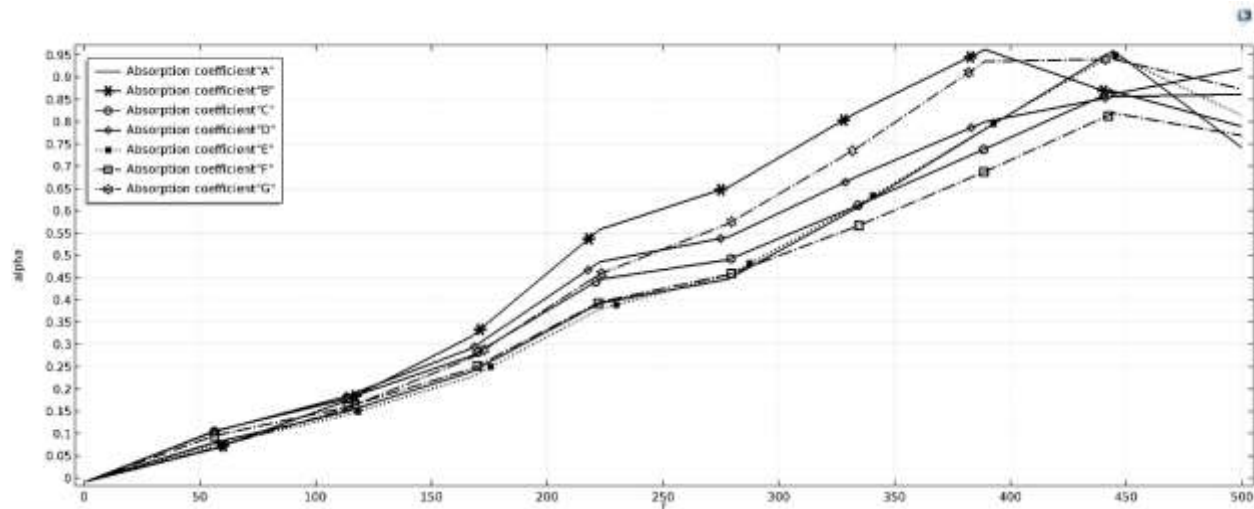


Fig. 10. Comparisons of all designs (shapes)

Figure 10 shows the results of the absorption coefficient of all designs in the form of a graph. As it can be seen, the best shape in terms of the coefficient of absorption was the concave shape “B”. The inverse pyramid “G” was in the next rank.

Calculating the Mpp effective area

Having considered all above results, the shaped plates

had a higher area than the flat plate, this may have increased the absorption coefficient rate of the shaped plates. In this section, the area of each of the plates was measured. For this reason, and due to the irregularities of the shapes, the effective area was defined. Then, the studied design was integrated to obtain the effective area of each of the shapes. The effective areas of each of the designs have been presented in Table 3.

Table 3. Effective area of different designs

Design	A	B	C	D	E	F	G
Effective area (m ²)	1	1.08	1.02	1.04	1.11	1.02	1.025

According to the Table 3 data, the shape E had the largest area and the shape A had the smallest area. The increased area was expected to cause an increase in absorption rate in these shapes. According to the results, it seems that such increase had not helped at least in the case of shape E, which had the highest area.

DISCUSSION

The improvement of the acoustic behavior of absorbent materials at low frequencies was an

important issue in the design of sound absorbers since the absorption of high frequency sound was often done well in the absorber materials. Also, the sound absorption rate approaches zero by decreasing the frequency, creating high-noise absorption at low frequencies was a goal for the manufacturers of sound absorbers. In Mpp, the energy losses of the acoustic wave occur by viscous heat losses inside the holes. When the air molecules travel through the holes, the inertia loss occurs. Compared to absorbent materials, Mpp has advantages such as lightness, less thickness, ease of washing, and sanitary issues. These benefits

have made it a proper alternative to absorbent materials. In this paper, the results of evaluating the acoustic performance of the shaped micro-perforated absorbers were presented. These results suggested that some of the shapes can increase the absorption rate in these adsorbents. In this regard, Y. Y. Lee evaluated the flexible curve-shaped micro-perforated panel, which ended up to an air chamber in the back. The results' of his study showed that the absorption coefficient of the micro-perforated panel improved by shaping it (curving) and got closer to the resonance frequencies [31]. Also, in a study by Sadeghi et al. on the effect of the pyramid angle in the perforated plates, three-angle vertices of 24, 29, and 36 degrees were examined. The results proved that the highest average absorption rates were respectively at a vertex angle of 36 °, at a frequency of 1000 Hz as 89.5%; at a vertex angle of 29 °, at a frequency of 900 Hz as 92%; and at a vertex angle of 24 °, at a frequency of 800 Hz as 93%. They also found that by decreasing the vertex angle of the pyramid and with the constant base area, the coefficient of absorption increases in the octave band frequencies and at frequencies below 1000 Hz. Additionally, the absorption peak shifts to low frequencies [32]. These results suggested the effect of the appearance on the absorption performance of absorbers and also confirmed the results of the present study.

Since the absorption factor was dependent on the frequency and the impact angle of the sound, thus, the absorber area had some effects on the absorption factor that the importance level of these factors needs to be determined [33]. To do so, 6 designs were defined as the surface shape of the micro-perforated plate, which were introduced to and defined in the three-dimensional environment of the COMSOL software considering the boundary conditions and proper relations. Given the graphs and the results presented, it was clear that the shape B had the best performance compared to shape "A" (reference) and the rest of the designs. The G, D, and C designs were ranked next in terms of increasing the absorption coefficient rate. The shape E had had exactly the absorption coefficient rate such as the reference shape. Finally, the shape F had had a worse absorption performance than the reference shape at some frequencies.

An explanation for this function was that the shaping of the micro-perforated plate creates a space

behind it with a variable height. Evaluating the shapes and considering Table 1, it can be seen that design B had the highest maximum height at the edges and the lowest height in the middle part. Although the designs were made in such a way that ultimately the effective height behind the micro-perforated plate remains constant in all shapes, however, the presence of space with such a height behind the micro-perforated plate causes resonance at some frequencies and may help to absorption phenomenon at some frequencies. The resonance frequency and the frequency band of the system depend on some parameters. For example, the diameter of the cavity represents the maximum absorption, while the thickness behind the plate represents the exact frequency of the maximum absorption. Although the presence of a variable-height space justifies the better performance of shape B compared to the reference shape but did not explain the performance of the rest of the shapes. Since in all defined cases, the presence of a shape on the plate creates a space with a variable height behind the micro-perforated plate, but their performances were different. The designs G and D had also equal maximum heights; however, the results showed that the performance of the shape G was better than the shape D. It was important to pay attention to the quality of the shapes to explain this kind of behavior. In the event of an acoustic wave encountering a non-flattened micro-perforated plate, a part of the wave enters the space behind due to the existence of cavities. The pores were suitable sound pathways at low frequencies due to the diffraction. The plate solid spaces reflected a shorter sound wavelength [34]. The waves entering through the perforated surface moved a pressure wave toward the bottom of the compartment, which will be also reflected upward after the collision with the bottom of the compartment, reaching the surface. These reflected waves had a phase difference with each other as the paths these had traversed and have not been the same due to the difference in depth. This causes constructive and potentially destructive interactions and makes changes in the rate of the absorption coefficient. On the other hand, when the soundwave hits a quite flat surface on a plate, it will be reflected in the same angle. When the flat surface changes, or in other words, becomes shaped or angled, a part of the energy is propagated in a direction other than the reflection angle. This propagation of and dispersion of the reflecting wave in

different directions is called diffusion [34-35]. Any non-flat surface can be considered a diffuser. The reflection mode or, in other words, the wave propagation in the back and front of the plate depends entirely on the shape of the plate. Hence, a design or shape leads to the concentration and directing the sound wave toward the absorbent surface, and as a result, increases the performance, while other designs cause the dispersion and distortion of the sound wave from the absorbent surface. The results of this study showed that, in general, the designs with a concave mode or regular or non-regular dents had a better coefficient of absorption than other designs and the reference design. In addition, the designs that were generally convex have shown a coefficient of absorption lower than the rest of the shapes and the reference design. The best example, in this case, was the G and D designs. The design G was almost concave and the shape D had a pyramidal and protruding state. Despite an equal maximum height, the shape G had a better absorption coefficient than the shape D. Another point was the dependence of the absorption coefficient on the sound wave angle. When the absorbent was so-called shaped, it will make the sound wave angled. Obviously, the absorption coefficient at some angles was more than other angles. Another issue to be mentioned in this regard was that the shaping of the absorbent surface increases the absorption area. The results of Table 3 showed that all defined shapes had more area than the typical shape (A). The maximum area was related to the shape E, where, the increased area relative to shape A was 0.11 square meters. It was expected that by an increasing the adsorbent area would contribute to the absorption phenomenon, while the results did not indicate such an outcome. In this regard, one may note that perhaps the increase in area has not been enough to be able to affect the absorption rate or, this factor depends entirely on the studied shape. In other words, if the examined shape geometrically contributes to the absorption phenomenon, the increase in the area will strengthen it; but in the shapes, in which geometry was as such that did not contribute to the absorption phenomenon, the increase in area would not be effective. However, in this study, the considered increase in the area showed no effect on increasing the absorption rate. Other shapes for further study can be examined.

CONCLUSION

1. Shaping creates a variable depth behind the micro-perforated plate. In other words, when a plate is shaped, the height behind it varies throughout the plate that creates resonance at some frequencies and may help to the absorption phenomenon at certain frequencies.
2. Shaping creates a phase difference and angling the sound wave. It also influences the reflection process that these factors affect the absorption coefficient.
3. Having shape increases the absorption area, which was expected to contribute to the absorption phenomenon. However, this factor seems not to be helpful in this study.

REFERENCES

1. [Cox TJ](#), [D' Antonio P](#). Acoustic Absorbers and Diffusers: Theory, Design and Application. Chapter 5. Spon Press. London and New York.2005
2. Nelson DI, Nelson RY, Concha-Barrientos M, Fingerhut M. The global burden of occupational noise-induced hearing loss. *Am J Ind Med*. 2005; 48:446-58. DOI:[10.1002/ajim.20223](#).
3. [Picard M](#), [Girard SA](#), [Simard M](#), [Larocque R](#), [Leroux T](#), [Turcotte F](#). Association of work-related accidents with noise exposure in the workplace and noise-induced hearing loss based on the experience of some 240000person-years of observation. *Accid Anal Prev*.2008; 40: 1644-1652. DOI: 10.1016/j.aap.2008.05.013.
4. [Ni CH](#), [Chen ZY](#), [Zhou Y](#), [Zhou JW](#), [Pan JJ](#), [Liu N](#), [Wang J](#), [Liang CK](#), [Zhang ZZ](#), [Zhang YJ](#). Associations of blood pressure and arterial compliance with occupational noise exposure in female workers of textile mill. *Chinese Med J*.2007; 120: 1309-1313. DOI: 10.1097/00029330-200708010-00003.
5. [Niemann H](#), [Bonney X](#), [Braubach M](#), [Hecht K](#), [Maschke C](#), [Rodrigues C](#), [Röbbel N](#). Noise-induced annoyance and morbidity results from the pan/European LARES Study. *Noise Health*. 2006; 8:9-32. DOI: 10.4103/1463-1741.33537.
6. [Dalton DS](#), [Cruickshanks KJ](#), [Klein BE](#), [Klein R](#), [Wiley TL](#), [Nondahl DM](#). The impact of hearing loss on quality of life in older adults.

- Gerontologist*. 2003; 43: 661 – 668. DOI: [10.2147/CIA.S26059](https://doi.org/10.2147/CIA.S26059).
7. [Kramer SE](#), [Kapteyn TS](#), [Kuik DJ](#), [Deeg DJ](#). The association of hearing impairment and chronic diseases with psychosocial health status in older age. *J Aging Health*. 2002; 14:122-137. [Doi.org/10.1177/089826430201400107](https://doi.org/10.1177/089826430201400107).
 8. [Babisch W](#). Transportation noise and cardiovascular risk: updated review and synthesis of epidemiological studies indicate that the evidence has increased. *Noise and Health*. 2006; 8:1-24. DOI: 10.4103/1463-1741.32464.
 9. [Berglund B](#), [Hassmén P](#), [Job RF](#). Sources and effects of low-frequency noise. *J Acoust Soc Am*. 1996; 5:2985-3002. DOI: 10.1121/1.414863.
 10. [Persson Waye K](#), [Bengtsson J](#), [Kjellberg A](#), [Benton S](#). Low frequency noise "pollution" interferes with performance. *Noise and Health*. 2001;4:33-49
 11. [Smith MG](#), [Croy I](#), [Ogren M](#), [Persson Waye K](#). On the influence of freight trains on humans: a laboratory investigation of the impact of nocturnal low frequency vibration and noise on sleep and heart rate. *PLoS One*. 2013; 8:e55829. DOI: 10.1371/journal.pone.0055829.
 12. [Fuchs, H.V.](#); [Zha, X](#). Micro-perforated structures as sound absorbers – a review and outlook. *Acta Acust united Ac*. 2006; 92:139–146.
 13. [Fuchs, H.V.](#); [Zha, X](#). Acrylic-glass sound absorbers in the plenum of the deutscher bundestag. *Appl Acoust*.1992; 51:211-217. [https://doi.org/10.1016/S0003-682X\(96\)00064-3](https://doi.org/10.1016/S0003-682X(96)00064-3).
 14. Gemin Li, Chris K Mechefske. A comprehensive experimental study of micro-perforated panel acoustic absorbers in MRI scanners. *Magn Reson Mater Phy*. 2010; 23:177-185. DOI: 10.1007/s10334-010-0216-9.
 15. Wu M Q. Micro-perforated panels for duct silencing, *NOISE CONTROL ENG J*. 1997; 45:69-77.DOI: 10.3397/1.2828428.
 16. Allam s, Abom m. A new type of muffler based on micro perforated tubes, *J. Vib. Acoust*. 2011;133.DOI:10.1115/1.4002956.
 17. [Heidi R V](#), [Pedro C](#), [Finn J](#). Optimization of multiple-layer micro perforated panels by simulated annealing. *Appl Acoust*. 2011;72:772-776.
 18. [Wang C](#), [Huang L](#), [Zhang Y](#). Oblique incidence sound absorption of parallel arrangement of multiple micro-perforated panel absorbers in a periodic pattern. *J Sound Vib*. 2014; 333:6828-6842. [DOI.org/10.1016/j.jsv.2014.08.009](https://doi.org/10.1016/j.jsv.2014.08.009).
 19. Maa D Y. micro perforated-panel wide band absorbers, *NOISE CONTROL ENG J*. 1987; 29:77-84. DOI: 10.3397/1.2827694.
 20. Lee D H, Kwon Y P. Estimation of the absorption performance of multiple layer perforated panel systems by transfer matrix method, *J Sound Vib*. 2004; 278:847-860. [DOI.org/10.1016/j.jsv.2003.10.017](https://doi.org/10.1016/j.jsv.2003.10.017).
 21. [Bravo T](#), [Maury C](#), [Pinhède C](#).Enhancing sound absorption and transmission through flexible multi-layer micro-perforated structures, *J Acoust Soc Am*. 2013; 134:3663-3673. DOI: 10.1121/1.4821215.
 22. Hashemi Z, Monazzam M R, Fahim A. Estimation of Sound Absorption Performance of Complex Perforated Panel Absorbers by Numerical Finite Element Method and examining the role of Different Layouts behind It. *FLUCT NOISE LETT* .2019; DOI: 10.1142/S0219477519500135.
 23. Lee Y Y, Lee E W M, Ng C. F. Sound absorption of a finite flexible micro-perforated panel backed by an air cavity, *J Sound Vib* . 2005; 287: 227-243. DOI: 10.1016/j.jsv.2004.11.024.
 24. [Chang D](#), [Liu B](#), [Li X](#). An electro mechanical low frequency panel sound absorber. *J Acoust Soc Am*. 2010; 128:639-645. DOI: 10.1121/1.3459838.
 25. Chen W H, Lee F C, Chiang D M. On the acoustic absorption of porous materials with different surface shapes and perforated plates. *J Sound Vib* .2000; 237:337-355. [DOI.org/10.1006/jsvi.2002.5113](https://doi.org/10.1006/jsvi.2002.5113).
 26. Easwaran V, Munjal M L Finite element analysis of wedges used in anechoic chambers. *J Sound Vib* .1993; 160:333-350. [DOI.org/10.1006/jsvi.1993.1027](https://doi.org/10.1006/jsvi.1993.1027).
 27. Kang Y J, Bolton J S. Finite element modeling for sound transmission through foam-lined double-panel structures. *J Acoust Soc Am*. 1996; 99:27555-2765.DOI: 10.1121/1.414856
 28. Tsay H S. Analysis of normal incidence absorption of pyramidal polyurethane foam by three-dimensional finite element frequency

- domain acoustical analysis. . *J Acoust Soc Am*. 2006; 120:2686. DOI: 10.1121/1.2354044.
29. Maa DY. Potential of micro perforated panel absorber, *J Acoust Soc Am*. 1998; 104:2861-2866. DOI.org/10.1121/1.423870.
 30. Keller J B, Givoli D. Exact non-reflecting boundary conditions. *J Comput Phys*. 1989; 82:172-192. DOI.org/10.1016/j.jcp.2003.09.006.
 31. Lee Y Y, Lee E W M. widening the sound absorption bandwidths of flexible micro-perforated curved absorbers using structural and acoustic resonances. *INT J MECH SCI*. 2007; 49:925-934. DOI.org/10.1016/j.ijmecsci.2007.01.008.
 32. Khavanin A, Sadeghi M, Mirzaei R, Safary A. The effect of apex angle on acoustic absorption coefficient in perforated sheet with pyramidal geometry. *Journal of Acoustical Engineering Society of Iran*. ۴(۱): 21-28. URL: <http://joasi.ir/article-1-70-fa.html>
 33. Ågren A. The design and evaluation of a hemi-anechoic engine test room. *Appl Acoust*. 1992; 37: 151-161. URL: <http://joasi.ir/article-1-70-fa.html>.
 34. Everest. F. A. Master Handbook of Acoustics .2001.
 35. Schroeder MR .Diffuse sound reflection by maximum length sequence. *J Acoust Soc Am*. 1975; 57:149- 50. DOI.org/10.1121/1.380425.
 36. Schroeder MR. Binaural dissimilarity and optimum ceilings for concert halls: more lateral sound. *J Acoust Soc Am*. 1979; 65:958-63. DOI.org/10.1121/1.382601.